applied sciences

MDPI

Article

Effect of Wood Fiber Loading on the Chemical and Thermo-Rheological Properties of Unrecycled and Recycled Wood-Polymer Composites

Klementina Pušnik Črešnar [1,*], Lidija Fras Zemljič [1], Lidija Slemenik Perše [2] and Marko Bek [2,*]

[1] Faculty of Mechanical Engineering, University of Maribor, 2000 Maribor, Slovenia; lidija.fras@um.si
[2] Faculty of Mechanical Engineering, University of Ljubljana, 1000 Ljubljana, Slovenia; lidija.slemenik.perse@fs.uni-lj.si
* Correspondence: klementina.pusnik@um.si (K.P.Č.); Marko.Bek@fs.uni-lj.si (M.B.); Tel.: +386-(2)-220-7607 (K.P.Č.)

Received: 14 November 2020; Accepted: 8 December 2020; Published: 11 December 2020

Abstract: Novel wood fiber (WF)-polypropylene composites were developed using the extrusion process with a twin-screw extruder. The influence of different mass addition of WF to unrecycled polypropylene (PP) and recycled PP (R-PP) on the chemical, thermal and rheological properties of the processed WF-PP and WF-R-PP composites was investigated. For this purpose, the chemical surface structure of the composites was followed with ATR-FTIR (attenuated total reflection Fourier transform infra red spectroscopy), while the thermal properties of the WF-PP composites were investigated with differential scanning calorimetry (DSC). Furthermore, the crystalline structure of the composites was determined by X-ray diffraction (XRD) analysis. Finally, the rheology of the materials was also studied. It was observed that a stronger particle formation at high additional concentrations was observed in the case of recycled PP material. The addition of WF over 20% by weight increased the crystallinity as a result of the incorporation and reorganization of the WF and also their reinforcing effect. The addition of WF to pure PP had an influence on the crystallization process, which due to the new β phase and γ phase PP formation showed an increased degree of crystallinity of the composites and led to a polymorphic structure of the composites WF-PP. From the rheological test, we can conclude that the addition of WF changed the rheological behavior of the material, as WF hindered the movement of the polymeric material. At lower concentrations, the change was less pronounced, although we observed more drastic changes in the material behavior at concentrations high enough that WF could form a 3D network (percolation point about 20%).

Keywords: wood-fiber; polypropylene; thermoplastic composites; highly filled; sustainable and biodegradable composites; rheological properties; ATR-FTIR; DSC; XRD

1. Introduction

The production of plastics has risen from two million tons in 1950 to 380 million tons in 2015 and is still increasing worldwide, causing serious environmental pollution [1–5]. The EU requirements and strategies encourage the reuse of plastics and promote high-quality plastics recycling processes [6,7]. Despite the fact that this area is an extremely hot topic and that much has been done, there is still room for specific plastics and a challenge for further advanced research.

Polypropylene (PP) is one of the most useful and manufactured plastics [8–10] and thus, a high treat for the environment, especially after the usage. Polypropylene's physical, chemical and mechanical properties, such as high stiffness, good tensile strength, chemical inertness to most diluted alkalis,

acids and solvents make this material extremely attractive for the use in different areas in the plastics and polymer materials industry. The growth market of PP includes industries such as appliance and consumer products, automotive, agriculture, construction, leisure, outdoor, sports, medical and healthcare, packaging, and fibers [1,11–13]. Due to its low density, it offers added value in weight-sensitive applications. Higher temperature resistance makes it suitable for objects such as trays, funnels, buckets, and bottles [14,15]. To reduce the environmental impact of PP, the focus of many studies is given toward the recycling and reuse of the PP. In the Society of the Plastics Industry, resin was defined so that PP could be recycled five times without changing its structural and mechanical properties [8].

Another interesting approach to PP sustainable use is the development of biodegradable PP composites. The biodegradability of PP composites can be increased by adding animal or mineral-based natural fibers to the neat polymer [3–5,7–10,16,17]. It has already been reported that, compared to animal fibers, the natural plant fibers are more suitable for the preparation of polymer composites, since they provide much higher strength and stiffness to the final material [4]. Natural fibers are easily recyclable, have low density and high specific strength and stiffness. The use of natural fibers as polymer reinforcement improves the flexural and tensile properties of pure polymers [18–23]. The fibers are prepared from renewable sources and therefore require less energy for the production. They are produced at lower costs as plastics and emit low quantities of toxic fumes. Using natural fibers is also beneficial in the manufacturing process since fibers tend to be less abrasive and cause less damage to processing equipment over time. Another benefit of using fibers is their low price, e.g., the price of wood flour is 0.09–0.18 € kg^{-1} compared to 1.04–1.43 € kg^{-1} for PP [4].

One of the important aspects of the plant fibers—polymer-based composites is the optimization of the interfacial bonding between the reinforcing plant fiber and polymer matrix, which leads to superior mechanical performance. It is known that; (i) the physical and chemical incompatibility between the fiber and matrix, leads to poor dispersion, weak interfacial adhesion and, ultimately, inferior composite quality; (ii) Inter-diffusion, electrostatic adhesion, chemical reactions and mechanical interlocking are, in general, responsible for the interfacial bonding and adhesion of plant fiber composites; (iii) A thorough knowledge of the structure-property relationship of the composite could be established by conducting a set of direct and indirect interfacial assessments. Thus, various modification approaches are required, aimed at overcoming the incompatibility and refining the interfacial adhesion of the composite, interfacial bonding mechanisms, and the assessment of interface structure and bonding [24].

One of the commonly used fibers related to the enhanced biodegradability of PP composites are wood fibers (WF). WF are composed of cellulose, hemicellulose, lignin, and extractives. Cellulose has the role of increasing the strength in WF because of its high crystallinity. Hemicellulose acts as a matrix for the cellulose and a connection between cellulose and lignin. The polyphenolic compound, lignin, acts as cement material. Because of its low density, low thermal expansion, renewability, and desirable mechanical strength, it is an appropriate material for the preparation of wood PP composites.

In general, incorporation of WF into the PP matrix affects the physical, chemical, and mechanical properties of the final product. With the incorporation of WF into the PP matrix, the biodegradability of WF-PP composites is enhanced [2]. There are many studies related to the development of wood (thermoplastics) polymer composites [2,14,16,17,25–29]. Common to these studies the production of wood-thermoplastic polymer composites is based on chemically treated wood or polymer, which results in enhanced interactions between the wood and thermoplastic material, and, as a consequence, improved properties, such as (i) increased degree of crystallinity, (ii) increased mechanical properties and (iii) improved rheological properties.

Several different physical approaches can be used to improve the interfacial bonding, such as corona, plasma treatment, heat treatments, electron radiation and fiber treatment. On the other hand, chemical approaches could be used as well, i.e., alkali, silane, benzyl, acryl, permanganate, peroxide, and malleated anhydride [9,14,30–32]. These chemical derivates are known: carboxymethylates,

benzoylates, urethanes, (meth) acrylates, maleated esters, isocyanates, ester resins and are mainly environmentally unfriendly and costly.

However, the presented research was focused on wood polymer composites prepared without modifications of WF or polymer, with the goal of obtaining good interfacial bonding and improved properties of PP material. Such an approach could be considered as "green", since only sustainable and biodegradable materials were used, which have less impact on the environment. Increased use of WF in the production of composites could also give a boost to the paper industry by providing an important new use of wood pulp, as WF can be derived from paper.

The goal of this paper was, therefore, to compare the chemical, thermal and rheological behavior of PP materials filled with wood fiber at different loadings without the use of additives. For the investigation, two PP matrix materials were used—recycled (R-PP), and unrecycled (PP) and their ability to form strong interfacial bonding between the wood fibers and polymer matrix was investigated.

2. Materials and Methods

2.1. Materials and the Preparation of Composite Materials

For the investigation, two different polypropylene matrix materials were used: unrecycled PP material AMPPLEO 1020 GA (0.94 g/cm^3, MFI: 20 g/10 min), Braskem, USA and recycled PP material Eco Meplen IC M20 BK (0.90 g/cm^3, MFI: 50 g/10 min) MEPOL S.r.l., Italy. Wood fibers were obtained locally from wood processing company as a side product of plywood grinding. The fibers consisted of spruce and pine wood, approximately in a ratio 80–20. Before mixing wood fibers with a polymeric matrix, the fibers were sieved to remove oversized wood particles.

All materials were prepared by melt compounding of polymeric matrix and wood fibers, without the use of additives. Before the extrusion, wood fibers, unrecycled PP and recycled PP were dried at 90 °C for 2 h in a ventilated oven. Wood fibers and PP were mixed and supplied to the feeder of the twin-screw extruder, PolyLab HAAKE Rheomex PTW 16, Thermo Haake, Germany. To assure uniform distribution of WF in the polymeric matrix, all materials were extruded four times. After each extrusion, the material was pelletized by a granulator, and the material was again fed to the feeder.

Altogether six materials were prepared with unrecycled PP matrix, and six with recycled PP matrix. Unrecycled PP and the recycled PP without the fibers were used as a reference, while other composites were prepared with wood fibers at different loading levels. A complete overview of the prepared materials is presented in Table 1, with designated names for each material mixture.

Table 1. Prepared materials and names of individual materials.

Wood Fiber Loading [wt.%]		**0**	**5**	**10**	**20**	**30**	**40**
Name of the material	Unrecycled PP	PP	WF-PP-5	WF-PP-10	WF-PP-20	WF-PP-30	WF-PP-40
	Recycled R-PP	R-PP	WF-R-PP-5	WF-R-PP-10	WF-R-PP-20	WF-R-PP-30	WF-R-PP-40

A melting temperature of around 190 °C was used for all materials and all four extrusion cycles. The screw speed was, in all cases, set to 80–90 rpm, and feeding was set to approximately 25 g/min of material. Measured average die temperatures of fourth extrusion cycle for the materials are presented in Table 2.

Table 2. Measured average die temperature in the PolyLab HAAKE Rheomex PTW 16 extruder.

Name of the Material	**PP**	**WF-PP-5**	**WF-PP-10**	**WF-PP-20**	**WF-PP-30**	**WF-PP-40**
Average die temperature [°C]	189.9	189.9	191.4	194.0	191.9	196.5
Name of the Material	**R-PP**	**WF-R-PP-5**	**WF-R-PP-10**	**WF-R-PP-20**	**WF-R-PP-30**	**WF-R-PP-40**
Average die temperature [°C]	189.9	189.9	191.4	194.0	191.9	196.5

Figure 1 shows the granules of all 12 investigated materials that were used in further investigation: ATR, (DSC), XRD and rheological tests.

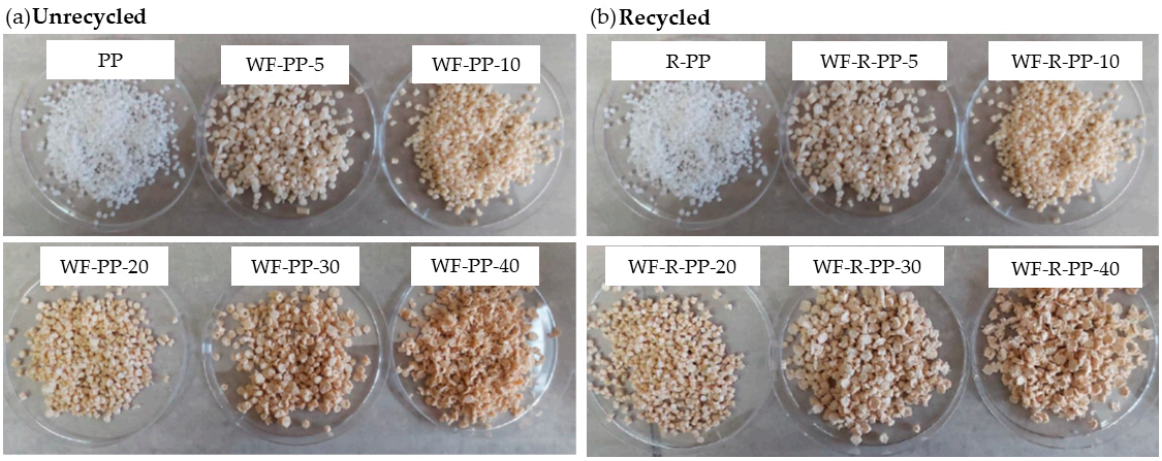

Figure 1. Granulated materials with different wt.% of wood fiber (WF) for unrecycled (**a**) and recycled (**b**) composite materials.

2.2. Experimental Methods

The volume size and volume size distribution of wood fibers were characterized using laser diffraction by a Particle Size Analyzer (PSA 1190), Anton Paar, Austria. To measure wood fiber sizes a particle-water suspension was first prepared. Before the measurement, the suspension was exposed to ultrasound for 30 s to break up potential wood fiber agglomerates. After this procedure, the measurements were conducted by exposing the flowing suspension to a laser beam for 10 s. Based on the diffracted light, particles sizes of wood fibers were determined, where the particle size is reported as a volume equivalent sphere diameter. This procedure was repeated seven times to determine the average size distribution of the particles.

For the investigation of the chemical structure, the ATR-FTIR spectra were performed using the Perkin Elmer Spectrum GX NIR FT-Raman. The sample was in contact with a diamond crystal. Each spectrum was determined as an average of 32 scans at a resolution of 4 cm^{-1} for the measuring background. Spectra of materials were measured in the range from 400 to 4000 cm^{-1} at room temperature. All spectra were baseline corrected and smoothed after the measurements.

Thermal properties of materials were investigated using differential scanning calorimetry, with a Mettler Toledo DSC 2 calorimeter. For the characterization, Al crucibles with a sample size between 10 and 30 mg were used. Tests were performed in an N_2 atmosphere, following the heat-cool-heat thermal cycle. Samples were first tempered at −65 °C for 5 min, followed by heating to 180 °C with the rate of 10 °C/min. This step was followed by the isothermal segment at 180 °C for 5 min, and cooling from 180 °C to −65 °C, again with the rate of 10 °C/min. The second heating cycle was repeated using the same conditions after isothermal segment at −65 °C.

Degree of crystallinity was evaluated by taking into account the actual content of the polymer in the composite following the Equation (1),

$$Xc = \frac{\Delta Hm}{\Delta H_0 f_{PP}} \times 100 \quad (1)$$

where X_C is the degree of crystallinity, Hm is the melting enthalpy, ΔH_0 is the melting temperature of the 100% crystalline PP and f_{PP} the weight fraction of PP in the composites. ΔH_0 for PP was found to be 209 (J/g).

The crystalline structure of composites was determined by X-ray diffraction (XRD) analysis, by a PANalytical PRO MPD diffractometer using a Cu Kα radiation source at 40 kV. The X-ray diffraction

patterns were recorded for the angles in the range of 2θ, from 10 to 40°, with a step of 10°/min (λ = 0.154 nm).

Rheological tests were performed by using a rotational rheometer, MCR 302 Anton Paar GmbH, Austria. Tests were performed with parallel plate sensor geometry, with sensor diameter 25 mm and gap 1 mm at constant temperature T = 190 °C. For the rheological characterization, the strain amplitude sweep and frequency sweep tests were performed. Two repetitions were made, and average values were calculated for each measurement. Strain amplitude sweep tests were performed at a constant frequency of 6.28 rad/s and increasing shear strain. The shear strain between γ = 0.01–100% was used for samples up to 20 wt.% of wood particles' loading, while for the samples with 30 wt.% and 40% wt.% of wood particles loading, the shear strain range was lower, i.e., between γ = 0.001–1%. Frequency sweep tests were performed in the frequency range from 0.062 to 628 rad/s at a constant shear strain. The value of strain was for each material selected in the linear viscoelastic (LVE) region of material behavior determined by the strain amplitude sweep tests. The shear strain γ = 0.1% was used for the samples with up to 20 wt.% wood fiber loading, while the shear strain γ = 0.01% was used for the samples with 30 wt.% and 40% wt.% of wood fiber loading.

3. Results

Figure 2 shows the size distribution of wood fibers measured by laser diffraction. As can be seen from optical microscopy, presented in the inserted image in Figure 2, the shape of the fiber was irregular and consisted of fibers, flakes and particles.

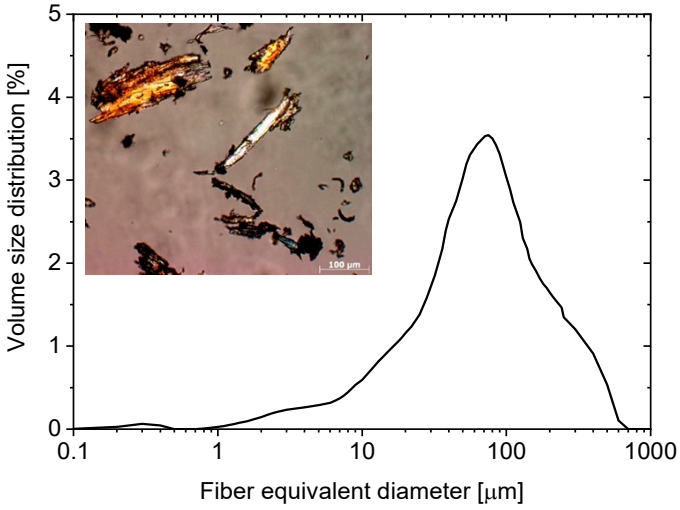

Figure 2. The volume size distribution of wood fibers.

Based on the measured wood fibers size distribution, the size parameters were evaluated and are presented in Table 3. The mean value of wood fiber was 99.58 μm. The distribution width of fiber sizes was evaluated through the D10, D50 and D90 values, which represents the values where 10%, 50% or 90% of the population lies below this percentage values. The additional parameter describing the width of size distribution is span, that was calculated as:

$$\text{Span} = \frac{\text{D90} - \text{D10}}{\text{D50}} \quad (2)$$

Table 3. Size parameters of wood fibers.

D10 [μm]	D50 [μm]	D90 [μm]	Mean [μm]	Span
12.16	63.67	221.23	99.58	3.28

Figure 3 shows the ATR-FTIR spectra of unrecycled PP (PP), recycled PP (R-PP) and wood fibers (WF) as reference samples. The characteristic bands of PP (black curve) and R-PP (red curve) at 2917 cm^{-1} correspond to CH_2 asymmetric stretching, the band at 2951 cm^{-1} to CH_3 stretching, and 2868 cm^{-1} to CH_2 asymmetric stretching. The characteristic peaks in the region at 1456 cm^{-1} and 1374 cm^{-1} were determined as CH_3 CH_2 rocking vibration. In the »fingerprint« region of PP and R-PP, the spectra contain several main PP tacticity, which include isotactic, syndiotactic and atactic forms. Typical characteristic peaks for isotactic PP are presented in the region below 1000 cm^{-1} [31]. The characteristic peaks for syndiotactic PP (s-PP) at 876 cm^{-1} and 808 cm^{-1} are shown in the spectra of R-PP and PP. The ATR-FTIR spectra of PP, R-PP indicate the presence of the mixture of isotactic and syndiotactic forms of PP.

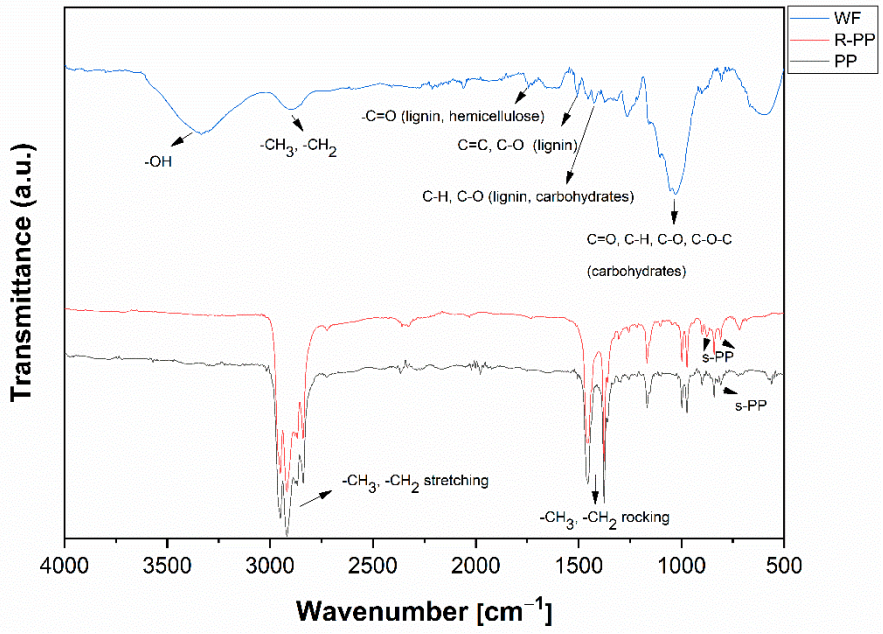

Figure 3. ATR-FTIR spectra of polypropylene (PP), recycled polypropylene (R-PP) and wood fiber (WF).

The characteristic vibration bands of WF (blue curve) are also shown in Figure 3. Wood fibers consist of cellulose, hemicellulose and lignin. Because the wood structure is very complex, the ATR-FTIR spectra were separated into two regions. The first region from, 3800 cm^{-1} to 2700 cm^{-1}, includes the OH and CH stretching vibrations. The second, at 1800 cm^{-1} to 800 cm^{-1}, is known as a »fingerprint« region for different functional groups of wood structures. A strong, broad peak can be seen at 3400 cm^{-1}, which was assigned to different O-H stretching, while, at 2950 cm^{-1}, a characteristic peak is related to the asymmetric and symmetric methyl and methylene stretching groups represented in wood. The »fingerprint« region of the wood consists of several bands which are related to the wood's structure. A characteristic peak assigned to C=O stretching vibration in lignin and hemicellulose could be observed at the 1741 cm^{-1}. The characteristic bands at 1505 cm^{-1} and 1270 cm^{-1} were determined as C=C, C-O stretching or bending vibrations of the groups in lignin. The bands at 1452 cm^{-1}, 1422 cm^{-1}, 1374 cm^{-1} were assigned to C-H, C-O deformation, bending or stretching vibrations of lignin groups and carbohydrates. The bands at 1165 cm^{-1}, 1050 cm^{-1}, 1030 cm^{-1} were assigned to C=O, C-H, C-O-C, C-O deformations or stretching vibrations of different groups in carbohydrates.

The peaks at 1030 cm^{-1} were assigned to C=O, C-H, C-O-C, C-O deformations or stretching vibrations of different groups in carbohydrates [10,33].

Figure 4 represents the ATR-FTIR spectra of unrecycled PP, recycled PP, WF and all wood fiber polypropylene composites with different concentrations of WF (from 5% of WF-PP-5 to 40% of WF-PP-40). The spectral analysis of unrecycled PP is shown in Figure 4a. From the spectra of WF-PP composites shown in this figure, the characteristic bands assigned to PP and wood structure could be

seen. The results showed that, with the addition of WF, a fingerprint characteristic band vibration appeared at 1030 cm^{-1} (assigned to the stretching vibrations of different groups in carbohydrates), at 1510 cm^{-1} (stretching or bending vibrations of groups in lignin), at 1741 cm^{-1} (stretching vibration in lignin and hemicellulose) and 3340 cm^{-1} (O-H stretching). Moreover, the intensity of vibration bands determined for wood structure increased with the increasing addition of wood fibers. The same characteristic vibration peaks of recycled PP (R-PP) and composites with different WF concentrations (WF-R-PP) are shown in Figure 4b. Spectral analysis showed (similarly as in the case of unrecycled PP and its composites) the presence of wood functional groups with their characteristic peaks at 1741 cm^{-1}, 1510 cm^{-1}, 1030 cm^{-1} and 3340 cm^{-1} assigned to the vibration of lignin, cellulose, and hemicellulose, and clearly suggesting the wood's presence on the surface of the material.

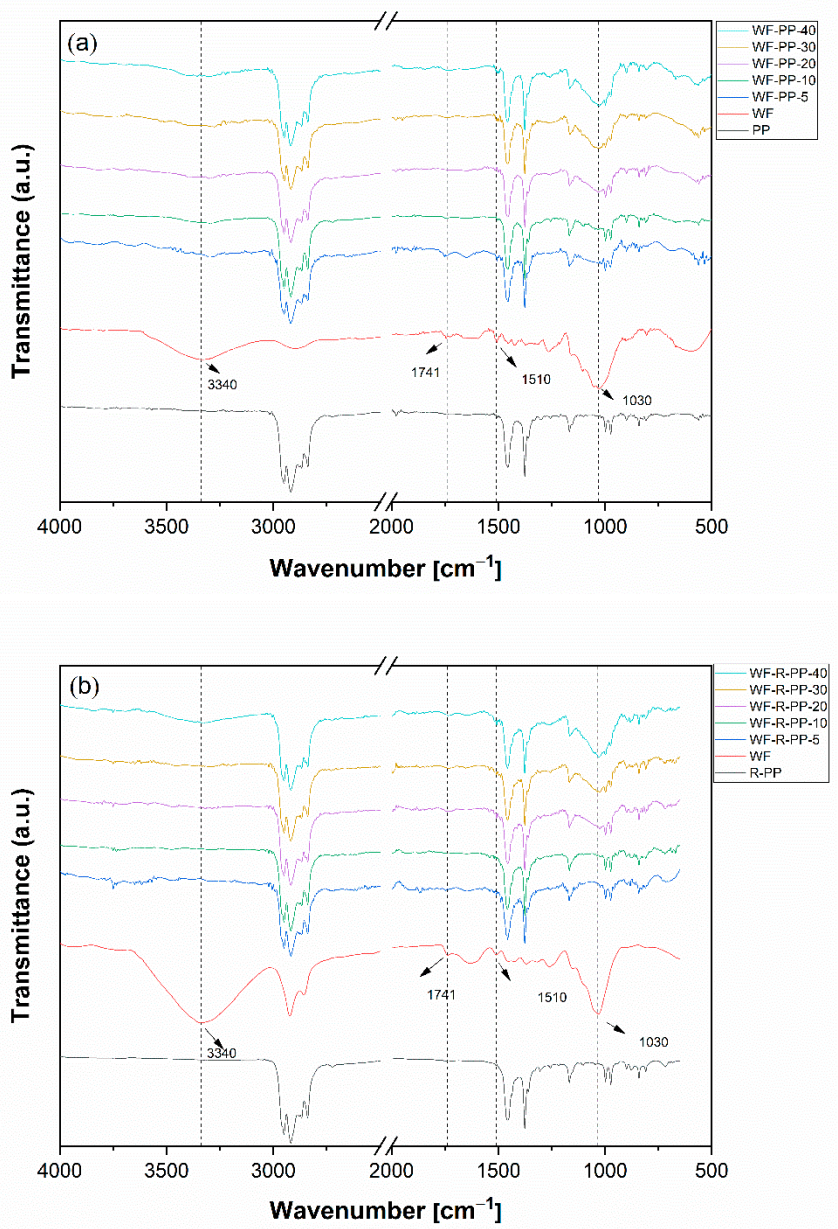

Figure 4. ATR-FTIR spectra of (**a**) unrecycled PP, WF, WF-PP composites and (**b**) recycled PP (R-PP), WF, WF-R-PP composites with different concentration of WF.

The spectra of PP based composites and R-PP based composites showed that there was no chemical interaction between the fibers and polymeric matrix. Since no treatment of wood fibers or compatibilizers were used, wood fibers act as fillers to the polymeric matrix.

To further investigate the influence of wood fibers, the thermal characterization of composites was performed. The effect of WF addition to a PP polymer has also been shown with thermal analysis of WF-PP and WF-R-PP composites. First, it was examined if WF had a role in the crystallization process of WF-PP composites. It is well known from the literature that WF has the role of a nucleating agent in the process of polymer crystallization, resulting in higher polymer crystallinity and increased mechanical properties of such composites [30,34]. However, treatment of WF or using the compatibilizers also affects the nucleating ability of WF. As the materials used in this study were not chemically treated and were not prepared by adding any additives the analysis of thermal properties enabled a direct comparison of the influence of fibers on the recycled and unrecycled materials.

To confirm the influence of the addition of WF to PP and R-PP on the nucleation ability of the composites, measurements of thermal properties were performed with differential scanning calorimetry (DSC) to examine the possible changes of crystalline properties between unrecycled and recycled PP/WF composites. The results of the thermal analysis are given in Table 4, where T_m is melting temperature, ΔH_m is melting enthalpy, Tc is the temperature of crystallinity and *Xc* is a degree of crystallinity. The measurements with unrecycled-PP and recycled-PP material showed that the melting temperature did not change significantly with increasing the amount of WF and was in all cases determined at around 165 °C. The thermal analysis of recycled PP (R-PP) exposed additional melting peak at around 117 °C. This peak indicated the thermal properties of polyethylene-origin materials and indicated that the recycled PP material contained some amount of PE polymer. However, since the melting enthalpy associated to this thermal transition was considerably smaller compared to the enthalpy related to the melting of PP, we may assume that the amount of PE polymer in the material was small and that it did not significantly affect the overall behavior of the (composite) material.

Table 4. Thermal parameters of the investigated composites.

Sample	Tm_1 (°C)	ΔHm_1 (J/g)	Tc (°C)	Tm_2 (°C)	ΔHm_2 (J/g)	*Xc* (%)
PP			130.32	166.32	86.49	41.4
WF-PP-5			130.85	166.81	89.40	45.1
WF-PP-10			129.65	166.67	87.80	46.7
WF-PP-20			126.91	166.30	75.86	45.4
WF-PP-30			123.64	165.90	66.98	45.8
WF-PP-40			122.05	165.27	61.37	48.9
R-PP	117.32	2.07	126.82	165.63	73.79	34.9
WF-R-PP-5	116.00	1.85	126.10	165.10	69.69	35.1
WF-R-PP-10	116.71	2.44	127.31	165.37	67.42	35.8
WF-R-PP-20	119.73	2.09	123.54	164.80	60.72	36.3
WF-R-PP-30	119.90	1.20	122.81	165.63	51.81	35.4
WF-R-PP-40	120.56	1.27	122.54	165.47	45.34	36.1

Abbreviations: T_m, melting temperature; ΔH_m melting enthalpy (1,2); Tc temperature of crystallinity; *Xc*, degree of crystallinity.

On the other hand, the addition of WF significantly changed the crystallization process of WF composites. The pure materials showed different degree of crystallinity. The unrecycled PP with 41.4% exhibited higher crystallinity (for about 19%) compared to recycled PP (R-PP) with 34.9%. The difference indicates a difference in the molecular structure of both materials. The degree of crystallinity increased with the addition of WF for both matrix materials (PP and R-PP). For PP based

composites, the degree of crystallinity increased from 41.4% to 48.9%, which represented an 18% increase. On the other hand, the degree of crystallinity of R-PP based composites increased from 34.9% to 36.1%, which represented only 3.5% increase.

These results showed that the addition of WF promoted crystallization process and confirmed that the fibers act as nucleating agents in the case of unrecycled PP matrix. The effect was less pronounced and marginal in the case of recycled based (R-PP) composites.

The temperature of crystallization of unrecycled PP was 3.5 °C higher compared to the unrecycled PP (R-PP). In Figure 5, the exothermic peaks represent the crystallization process of PP (Figure 5a) and R-PP (Figure 5b). The temperature of crystallinity was also affected by the addition of wood fibers. Compared to pure PP, the Tc of WF-PP-40 composite was 8 °C lower, i.e., at 122 °C, which represented about 6 % decrease of Tc when the highest amount of WF was added to pure PP. A similar decrease in crystallization temperature was also obtained for recycled based (R-PP) composites. The temperature of crystallization decreased from 126.82 °C for R-PP material to 122.54 °C for WF-R-PP-40 composite material. In this case, the difference was about 3%.

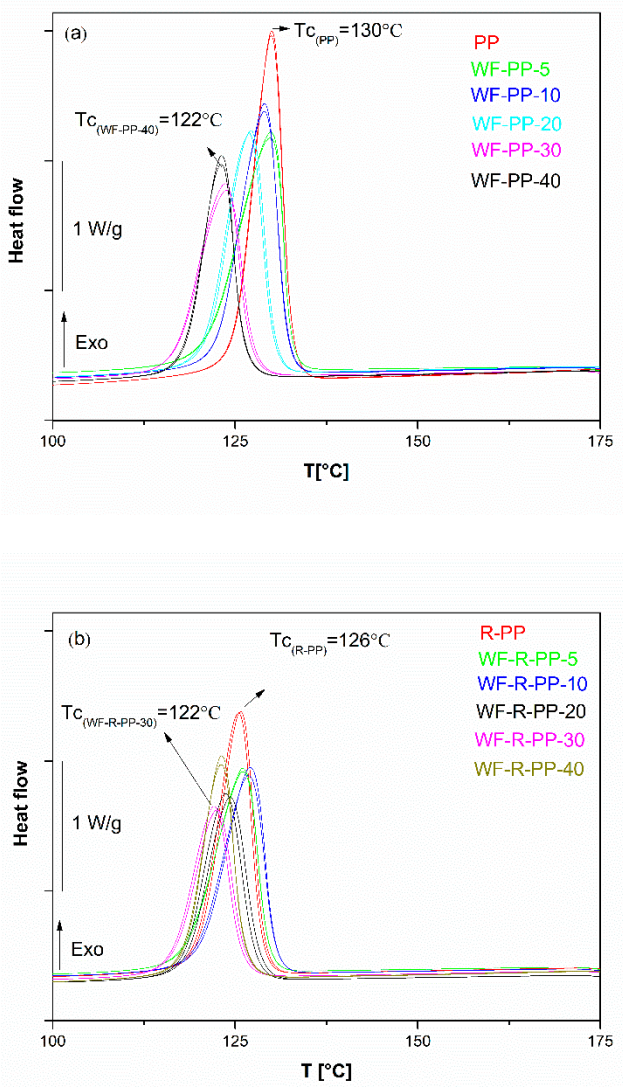

Figure 5. Differential scanning calorimetry (DSC) thermograms of (**a**) WF-PP composites and (**b**) WF-R-PP composites.

These results are in line with the results of the degree of crystallinity, as they show that the addition of wood fiber significantly affects the crystallization process of PP based composites. The addition of

WF has a lesser effect on the temperature of crystallization of R-PP based composites. In the literature, we can find information on the nucleation ability of lignocellulosic materials such as WF [25,27,30]. The researchers reported that untreated WF in thermoplastic composites act as good nucleating agents, while different chemical treatment of WF can lead to either increased or decreased nucleating ability. For example, the chemical modification of the fillers that causes smoothing of the filler surface leads to lower nucleation ability. In the case of composite investigated within this study, we were dealing with untreated wood fibers; however, they exhibited different nucleating ability depending on the used matrix material.

To further investigate the effects of fillers and their role as nucleating agents, XRD measurements coupled with X-ray diffraction were performed to obtain a detailed picture of the nature of the crystallographic structures. It is known that the presence of some fillers with nucleating ability leads to the formation of the β-form in PP [35–37]. WF as natural fillers are responsible for the changes in the crystallinity process and morphology. PP crystalize predominately in the α-monoclinic form by isothermal crystallization. The β-hexagonal, γ-triclinic phases and sematic modifications, all with a 3_1-helix conformation, may be crystallized from the melt under high undercooling or high-pressure conditions, or by the addition of nucleating agents. The α-monoclinic form is one of the thermodynamically stable crystalline modifications. Several researchers have already reported that α-monoclinic forms of PP are more brittle, while β-forms are ductile up to large strains [3,38,39].

Consequently, the further investigation was focused on the analysis of morphology changes of WF-PP and WF-R-PP composites determined with XRD measurements. In addition, X-ray diffraction was used to obtain more details about the nature of the crystallographic structure of WF-PP and WF-R-PP composites as a result of added WF. The X-ray diffraction results showed the influence of WF PP matrix addition on the polymorphism of the prepared WF-PP composites.

The diffractograms of unrecycled PP and WF-PP composites with various amount of WF are presented in Figure 6. The diffraction peaks for PP are positioned at 2θ angles of 13.9° (110), 16.8° (004), 18.5° (130), 21.4° (111) and 28.6° (200). All these peaks reflect the α-crystalline phase of PP. On the other hand, the diffraction peaks of WF-PP composites were determined at 2θ angles of 13.4° (110) and 18° (130), which revealed the α-crystalline phase of PP. The diffraction peaks positioned at 2θ angles of 16.3° (020), 21° (121), 28.1° (012) reflected the β-phase, and 14.9° (113) determined the γ-phase. By increasing the wt.% of WF the intensity of β-phase and γ-phase of PP increased, resulting in a polymorphic structure of the WF-PP composites.

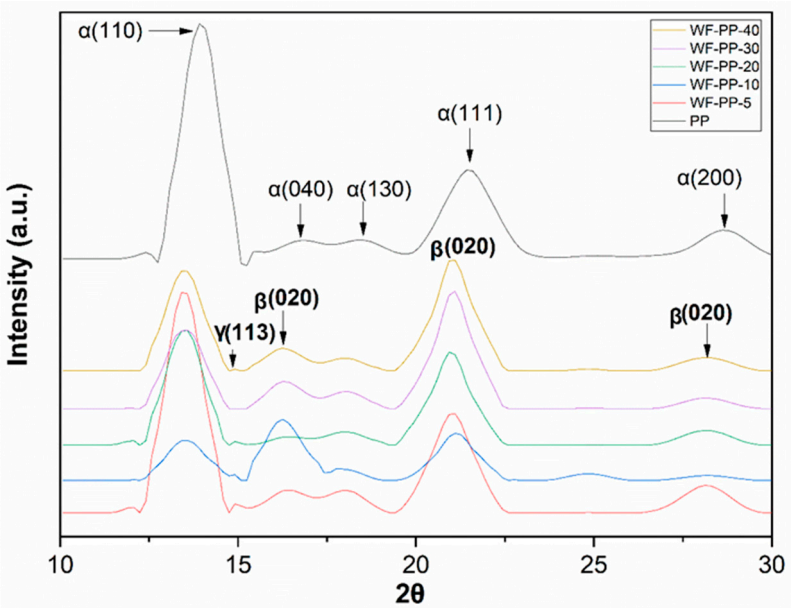

Figure 6. X-ray diffraction patterns of PP and WF-PP composites.

Figure 7 shows the diffractograms of recycled PP (R-PP) and WF-R-PP composites. Comparing the results of R-PP matrix to the composites at all loading levels shows that there are no differences in diffraction peaks, and there is no evidence of any phase transformation. Diffraction peaks for the α-crystalline phase of R-PP and all WF-R-PP composites were positioned at 2θ angles of 13.9° (110), 16.8° (004), 18.5° (130), 21.4° (111) and 28.6° (200).

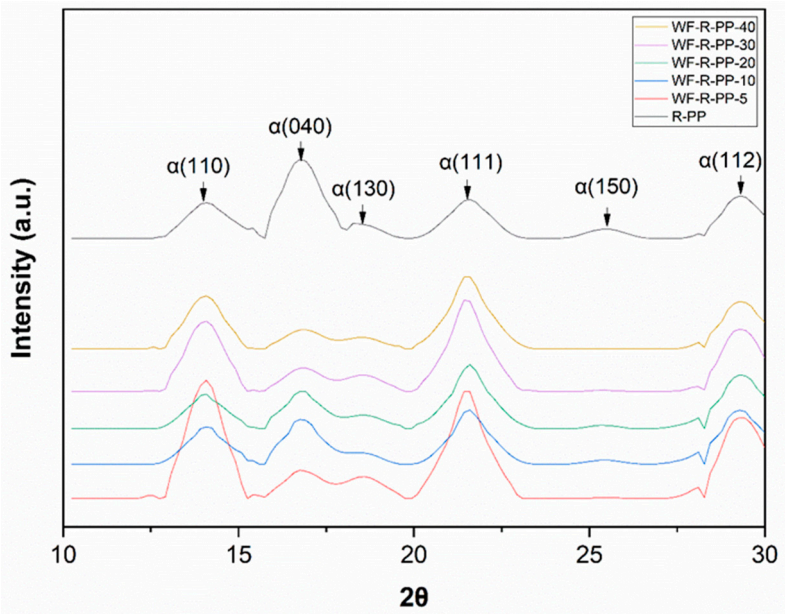

Figure 7. X-ray Diffraction patterns of R-PP and WF-R-PP composites.

The introduction of WF in the PP matrix resulted in the additional formation of the another two of the most prominent phases of PP, β and γ-phases. The formation of the well-known β-phase in PP composites has been in the literature explained with the first kinetic aspect of β-structure formation. Another reason for β-phase formation is related to the modification of wood filler. In detail, researchers who studied PP composites with sisal fibers, and another who studied PP composites with flax and Kevlar fibers, explained the formation of the β-phase through the occurring addition of any types of fillers. That means that fillers' increased roughness resulted in the presence of higher shear forces, which are responsible for the β-phase of PP formation [40–43].

In contrast, for recycled based composites (WF-R-PP) only the main α-crystalline phase of PP was detected, and the addition of wood fibers had no effect on the modification of the crystalline structure.

From the presented results, it is clear that the interaction between the fibers and the polymeric matrix is different for pure PP and recycled PP (R-PP) materials. A handy tool for understanding the filler—polymer interaction is melt rheology. Figure 8 shows the results of the strain sweep experiments for both matrix materials (PP and R-PP) and the corresponding composites. All materials exhibited a linear behavior at low strains, followed by non-linear behavior, where storage modulus dropped considerably from constant values. As the shear strain increased, polymer molecules started to disentangle, which lead to the decrease of storage modulus as the strain was increased. For the unrecycled PP and recycled PP (R-PP) the change from linear to non-linear behavior occurred at shear strain around $\gamma \sim 0.1$. Similar behaviour was also observed for composites with 5 and 10 wt.% WF concentrations. This indicates that the presence of fibers did not significantly affect the disentanglement process of polymeric molecules.

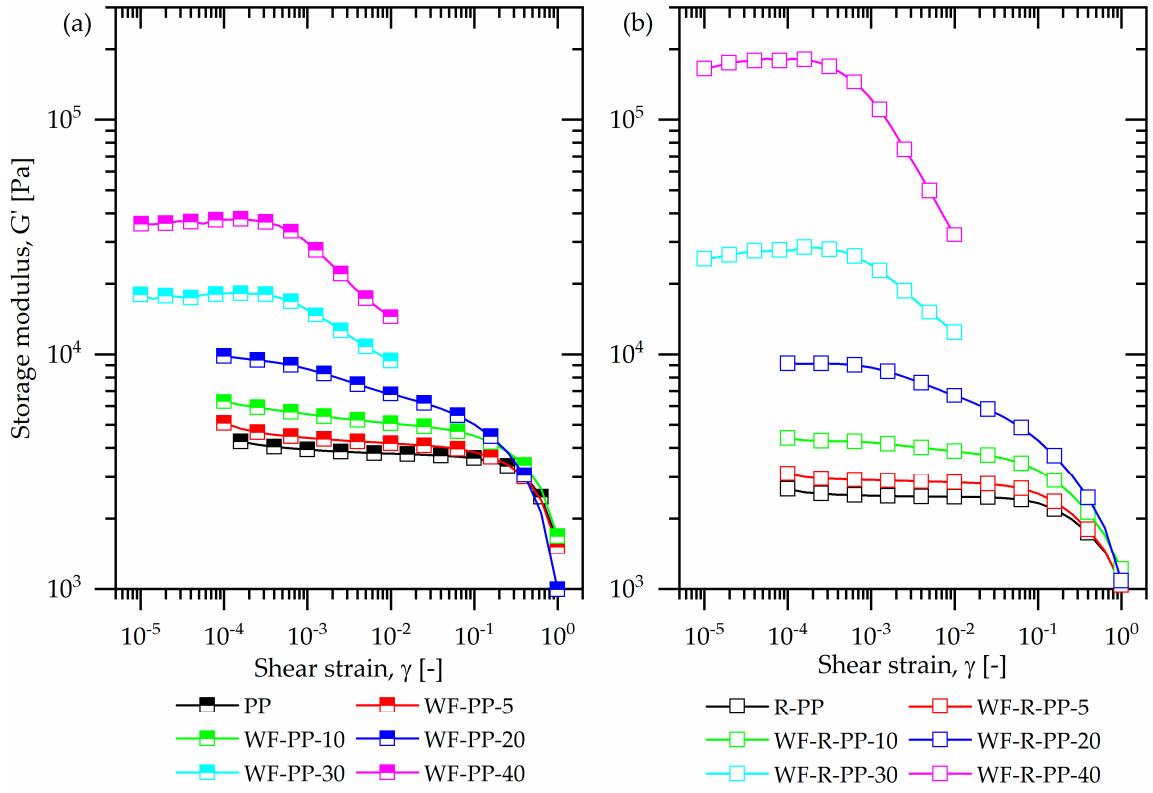

Figure 8. Storage modulus, G′ as a function of shear strain, γ at 6.28 rad/s and 190 °C for (**a**) unrecycled material and (**b**) recycled material.

A more gradual decrease of storage modulus was observed for the composites with filler loading higher than 20 wt.%. As the wood fiber concentration increases, a percolation point is reached, where wood fibers start to interact with each other directly and form a 3D network. With increasing shear strain, this fiber network is impaired, which results in a decrease in storage modulus. This process occurs at lower shear strains compared to strain values where polymer molecules disentangle. Consequently, the change from linear to non-linear behavior for the composites with 30 and 40 wt.% of wood fiber, occurred at very low strain $\gamma \sim 0.001$. In this respect, no significant differences were observed between the recycled and unrecycled composite materials.

The addition of relatively rigid (compared to molten polymer) WF to the polymer matrix, the elasticity of composite materials increased. This can be seen as an increase in storage modulus with the increasing concentration of wood fiber. This behavior has already been well-reported and observed for other types of polymer-fiber composites as well [44,45]. From Figure 8 it can be seen that the increase of storage modulus with the increasing concentration of wood fiber was more pronounced for R-PP polymeric matrix (Figure 8b). These results suggest that, for the recycled material (R-PP), a stronger WF network was formed at concentrations higher than 20%, resulting in higher values of storage modulus.

Following the amplitude sweep test, the frequency tests were performed in the linear viscoelastic region (Figure 9). For both cases, the R-PP and PP based composites, it is evident that the addition of WF up to 10 wt.% had no or limited influence on the rheological behavior of the melts in linear viscoelastic range. The values of storage and loss modulus over the entire frequency range were for pure PP and R-PP materials very comparable. Above this WF concentration, it seems that fibers start to interact. This is evident by an increase of values of the dynamic material function and especially by the material behavior at low frequencies where fiber-fiber interactions are dominant [45]. For composites up to 20 wt.% the hydrodynamic effects of the polymer matrix becomes dominant at higher frequencies.

In this region, the values of dynamic material functions regardless of the filler concentration were very similar.

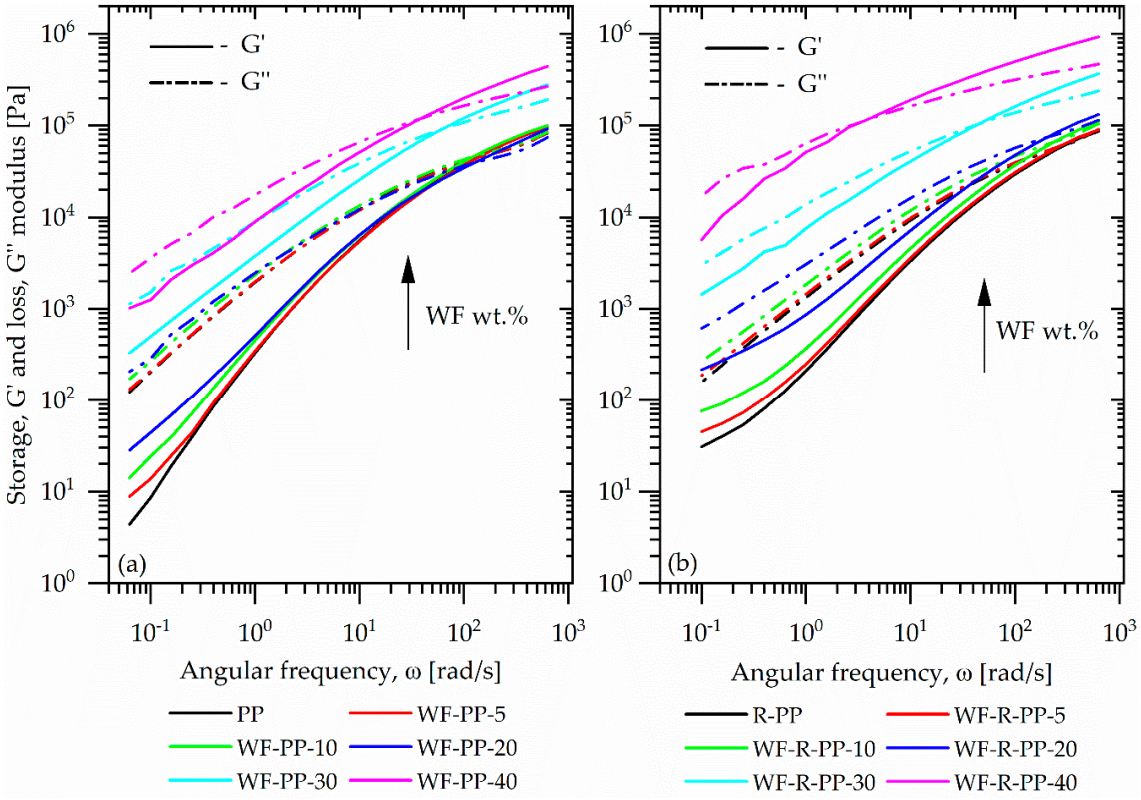

Figure 9. Storage G′ and loss G″ modulus as a function of angular frequency at 190 °C for (**a**) unrecycled material and (**b**) recycled material in the linear viscoelastic region.

A more substantial change of dynamic properties compared to the pure PP and R-PP can be observed at composites with 30 and 40 wt.% of fillers for PP based composites and for 20, 30 and 40 wt.% for R-PP based composites. The increased values of dynamic properties were contributed to the wood fiber network formation that resulted in higher storage and loss modulus and showed that the strong interactions between the polymer and the fiber occurred at higher concentrations. Comparison between the matrix materials also showed that the addition of WF had a significant effect on the rheological behavior of the recycled PP (R-PP), as it resulted in higher dynamic moduli compared to PP based composites.

Moreover, the results in Figure 9 show that wood concentration affected the viscoelastic character of the materials. This is evident by the crossover between G′ and G″ and was analyzed separately in Figure 9 for all composites.

From Figure 10 it can be seen that with the increasing WF concentration the crossover point shifted to lower frequencies, meaning that frequency range with solid-like (G′ > G″) material behavior broadens. Up to 20 wt.% of WF, the frequency of transition gradually decreased with increasing fiber concentration. Up to this concentration, the frequency of transition was also higher for the recycled material. At 30 wt.% and above a more drastic change of crossover point is seen, especially in the case of recycled material. In the case of the composite with 40 wt.% of WF with recycled material (WF-R-PP-40), the liquid to solid-like behavior occurred at frequency 3.7 rad/s, while for pure matrix material (R-PP) this transition was observed at 300 rad/s. These results confirmed that as the wood fiber network was formed, it significantly affected the dynamic mechanical properties of the composite materials.

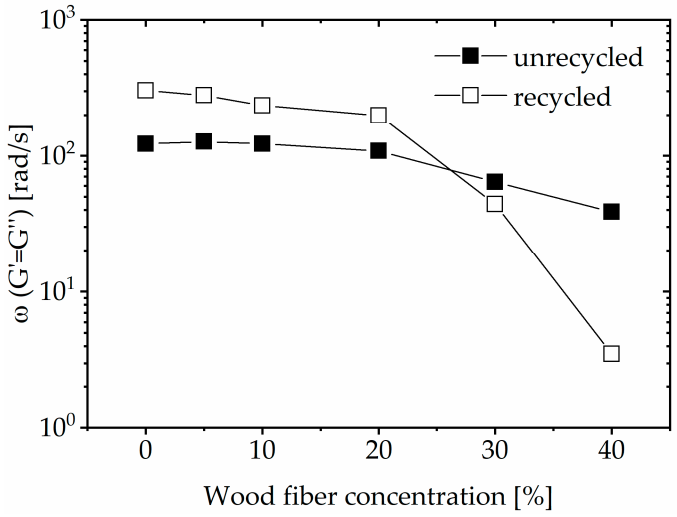

Figure 10. Crossover point at 190 °C for unrecycled (WF-PP) and recycled (WF-R-PP) materials.

4. Discussions with Conclusions

In this paper, the effect of the recycling of PP based wood fiber composites was investigated. As no additives or any kind of chemical fiber treatment was used, the investigation provides the information on the direct polymer—fiber interaction and effects of wood fiber loading. The interactions were evaluated through chemical, thermal and rheological characterization.

The ATR-FTIR spectra of all investigated composite materials showed the presence of basic functional wood groups with their characteristic peaks at 1741 cm^{-1}, 1510 cm^{-1}, 1030 cm^{-1} and 3340 cm^{-1}, which were determined for the vibration of lignin, cellulose and hemicellulose. No chemical interactions between the fibers and matrix material were observed, which was expected since no compatibilizers were used in the preparation of composite materials.

The thermal analysis showed that increasing the WF concentrations increased the degree of crystallinity as wood fibers acted as nucleating agents. While the increase in crystallinity for R-PP based composites was modest (maximal 3.5% increase), the increase in the case of PP based composites was much more decisive. The crystallinity of PP based composite with 40 wt.% of WF increased by 18%. As none of the matrix materials formed chemical bonds with the filler, the increased crystallinity of PP based composites may be related to the molecular structure of the polymer. The values of crystallinity at all loading levels were for R-PP based composites lower compared to PP based composites. This might be a consequence of branched polymeric structure or lower molecular weight of the recycled PP.

Additionally, to the increased crystallinity of PP based composites, the XRD measurements showed the formation of all three PP crystalline phases that were not present in pure PP material. In the case of R-PP based composites, PP α-crystalline phase was unchanged regardless of the WF loading.

This leads to an interesting observation. A substantial increase of crystallinity and additional crystalline phases appeared with PP based composites. Both lead to increased mechanical properties, such as elastic modulus and toughness of the material. It was shown that the addition of WF reinforced the PP material and to a lesser extent, also the recycled PP material. However, rheological characterization showed the opposite trend. At concentrations, which were high enough that wood fibers formed a 3D connected network, dynamic rheological properties increased considerably compared to the pure matrix materials. The strength of this wood fiber network was determined by the magnitude of the dynamic moduli. For example, comparing the loss modulus of pure PP with loss modulus of 40wt.% filled material showed a maximal increase of modulus for about 20%. However, for the R-PP based composites, the reinforcing effect was much larger as the modulus increased by about 110%.

In conclusion, it seems that there are two mechanisms controlling the behavior of WF filled composites. In the case of PP based composites, wood fibers promote the crystallinity and have no or limited effect on R-PP based composites. On the other hand, the R-PP based composites form strong

wood particle networks. Which mechanism will have a more significant effect on the mechanical properties is currently still unknown and should be a subject of further research.

Nevertheless, the results of this research showed that combining PP or R- PP with natural waste materials, such as wood fibers leads to improved thermal and rheological properties, which could be further improved with the use of compatibilizers or chemical treatment of wood fibers.

Author Contributions: Conceptualization, K.P.Č. and M.B.; methodology, K.P.Č.; formal analysis, K.P.Č., M.B.; investigation, K.P.Č., L.F.Z.; M.B.; writing—original draft preparation, K.P.Č., M.B.; writing—review and editing, K.P.Č., M.B., L.F.Z.; supervision, L.F.Z., L.S.P.; visualization, K.P.Č., M.B.; writing—original draft, K.P.Č., M.B.; writing—review and editing, K.P.Č., M.B., L.F.Z., L.S.P. All authors have read and agreed to the published version of the manuscript.

Funding: This work was financially supported by the Slovenian Research Agency in a frame of project P2-0264 and the research core funding of Ministry of education, science, and sport no. OP20.04343. Funding through the Research Programs P2-0118, of the Slovenian Research Agency (ARRS) is also gratefully acknowledged.

Acknowledgments: Authors acknowledge the MLINAR d.o.o., Slovenia for the in-kind donation of wood fibers for research purposes. We would also like to acknowledge Plastika Skaza d.o.o, Slovenia for sharing unrecycled and recycled PP material.

Conflicts of Interest: The authors declare no conflict of interest. The funders had no role in the design of the study; in the collection, analyses, or interpretation of data; in the writing of the manuscript, or in the decision to publish the results.

References

1. Ibeh, C.C. *Thermoplastics Materials Properties, Manufacturing Methods and Applications*; CRS Press Taylor and Francis Group: Boca Raton, FL, USA, 2011.
2. Mattos, B.D.; Misso, A.L.; De Cademartori, P.H.; De Lima, E.A.; Magalhães, W.L.E.; Gatto, D.A.; De Cademartori, P.H.G. Properties of polypropylene composites filled with a mixture of household waste of mate-tea and wood particles. *Constr. Build. Mater.* **2014**, *61*, 60–68. [CrossRef]
3. Butylina, S.; Hyvärinen, M.; Kärki, T. A study of surface changes of wood-polypropylene composites as the result of exterior weathering. *Polym. Degrad. Stab.* **2012**, *97*, 337–345. [CrossRef]
4. Pickering, K.L.; Efendy, M.G.A.; Le, T.M. A review of recent developments in natural fibre composites and their mechanical performance. *Compos. Part A Appl. Sci. Manuf.* **2016**, *83*, 98–112. [CrossRef]
5. Kang, Y.-A.; Kim, K.-H.; Ikehata, S.; Ohkoshi, Y.; Gotoh, Y.; Nagura, M.; Urakawa, H. In-situ analysis of fiber structure development for isotactic polypropylene. *Polymer* **2011**, *52*, 2044–2050. [CrossRef]
6. Flieger, M.; Kantorová, M.; Prell, A.; Řezanka, T.; Votruba, J. Biodegradable plastics from renewable sources. *Folia Microbiol.* **2003**, *48*, 27–44. [CrossRef]
7. Ojeda, T.; Freitas, A.; Birck, K.; Dalmolin, E.; Jacques, R.; Bento, F.; Camargo, F. Degradability of linear polyolefins under natural weathering. *Polym. Degrad. Stab.* **2011**, *96*, 703–707. [CrossRef]
8. Herrera, N.; Mathew, A.P.; Oksman, K. Plasticised polylactic acid/cellulose nanocomposites prepared using melt-extrusion and liquid feeding: Mechanical, thermal and optical properties. *Compos. Sci. Technol.* **2015**, *106*, 149–155. [CrossRef]
9. Fabiyi, J.S.; Mcdonald, A.G. Composites: Part a Effect of wood species on property and weathering performance of wood plastic composites. *Compos. Part A* **2010**, *41*, 1434–1440. [CrossRef]
10. Poletto, M. Thermal degradation and morphological aspects of four wood species used in lumber industry. *Rev. Árvore* **2016**, *40*, 941–948. [CrossRef]
11. Farzi, A.; Dehnad, A.; Fotouhi, A.F. Biodegradation of polyethylene terephthalate waste using Streptomyces species and kinetic modeling of the process. *Biocatal. Agric. Biotechnol.* **2019**, *17*, 25–31. [CrossRef]
12. Ogunsona, E.O.; Codou, A.; Misra, M.; Andrzejewski, J. A critical review on the fabrication processes and performance of polyamide biocomposites from a biofiller perspective. *Mater. Today Sustain.* **2019**, *5*, 100014. [CrossRef]
13. Prambauer, M.; Wendeler, C.; Weitzenböck, J.; Burgstaller, C. Biodegradable geotextiles–An overview of existing and potential materials. *Geotext. Geomembranes* **2019**, *47*, 48–59. [CrossRef]
14. Iwamoto, S.; Yamamoto, S.; Lee, S.-H.; Endo, T. Mechanical properties of polypropylene composites reinforced by surface-coated microfibrillated cellulose. *Compos. Part A Appl. Sci. Manuf.* **2014**, *59*, 26–29. [CrossRef]

15. Cheng, W. Preparation and properties of lignocellulosic fiber/$CaCO_3$/thermoplastic starch composites. *Carbohydr. Polym.* **2019**, *211*, 204–208. [CrossRef]
16. Mehta, S.; Mirabella, F.M.; Rufener, K.; Bafna, A. Thermoplastic olefin/clay nanocomposites: Morphology and mechanical properties. *J. Appl. Polym. Sci.* **2004**, *92*, 928–936. [CrossRef]
17. Jain, K.; Madhu, G.; Bhunia, H.; Bajpai, P.K.; Nando, G.B.; Reddy, M.S. Physico-mechanical characterization and biodegradability behavior of polypropylene/poly(L-lactide) polymer blends. *J. Polym. Eng.* **2015**, *35*, 407–415. [CrossRef]
18. Tribot, A.; Amer, G.; Alio, M.A.; De Baynast, H.; Delattre, C.; Pons, A.; Mathias, J.-D.; Callois, J.-M.; Vial, C.; Michaud, P.; et al. Wood-lignin: Supply, extraction processes and use as bio-based material. *Eur. Polym. J.* **2019**, *112*, 228–240. [CrossRef]
19. Sienkiewicz, M.; Janik, H.; Borzędowska-Labuda, K.; Kucińska-Lipka, J. Environmentally friendly polymer-rubber composites obtained from waste tyres: A review. *J. Clean. Prod.* **2017**, *147*, 560–571. [CrossRef]
20. Rowell, R.M.; Sanadi, A.R.; Caulfield, D.F.; Jacobson, R.E. Utilization of Natural Fibers in Plastic Composites: Problems and Opportunities. *Lignocellul. Compos.* **1997**, *13*, 23–51.
21. Li, X.; Tabil, L.G.; Panigrahi, S. Chemical Treatments of Natural Fiber for Use in Natural Fiber-Reinforced Composites: A Review. *J. Polym. Environ.* **2007**, *15*, 25–33. [CrossRef]
22. Taj, S.; Munawar, M.A.; Khan, S. Natural fiber-reinforced polymer composites natural fiber-reinforced polymer composites. *Pakistan Acad. Sci.* **2007**, *44*, 129–144.
23. Pracella, M.; Haque, M.-U.; Alvarez, V. Functionalization, Compatibilization and Properties of Polyolefin Composites with Natural Fibers. *Polymer* **2010**, *2*, 554–574. [CrossRef]
24. Zhou, Y.; Fan, M.; Chen, L. Interface and bonding mechanisms of plant fibre composites: An overview. *Compos. Part B Eng.* **2016**, *101*, 31–45. [CrossRef]
25. Wang, K.; Bahlouli, N.; Addiego, F.; Ahzi, S.; Rémond, Y.; Ruch, D.; Muller, R. Effect of talc content on the degradation of re-extruded polypropylene/talc composites. *Polym. Degrad. Stab.* **2013**, *98*, 1275–1286. [CrossRef]
26. Paik, P.; Kar, K.K. Polypropylene nanosphere: Particle size and crystal structure. *Int. J. Plast. Technol.* **2009**, *13*, 68–82. [CrossRef]
27. Akbar, D. Surface modification of polypropylene (PP) using single and dual high radio frequency capacitive coupled argon plasma discharge. *Appl. Surf. Sci.* **2016**, *362*, 63–69. [CrossRef]
28. Saujanya, C.; Radhakrishnan, S. Structure development and crystallization behaviour of PP/nanoparticulate composite. *Polymer* **2001**, *42*, 6723–6731. [CrossRef]
29. Sevegney, M.S.; Kannan, R.M.; Siedle, A.R.; Percha, P.A. FTIR spectroscopic investigation of thermal effects in semi-syndiotactic polypropylene. *J. Polym. Sci. Part B Polym. Phys.* **2005**, *43*, 439–461. [CrossRef]
30. Borysiak, S.; Grząbka-Zasadzińska, A.; Odalanowska, M.; Skrzypczak, A.; Ratajczak, I. The effect of chemical modification of wood in ionic liquids on the supermolecular structure and mechanical properties of wood/polypropylene composites. *Cellulose* **2018**, *25*, 4639–4652. [CrossRef]
31. Zheng, K.; Liu, R.; Chang, H.; Shen, D.; Huang, Y. In situ FTIR spectroscopic study of the conformational change of syndiotactic polypropylene during the isothermal crystallization. *Polymer* **2009**, *50*, 5782–5786. [CrossRef]
32. He, P.; Xiao, Y.; Zhang, P.; Xing, C.; Zhu, N.; Zhu, X.; Yan, D. Thermal degradation of syndiotactic polypropylene and the influence of stereoregularity on the thermal degradation behaviour by in situ FTIR spectroscopy. *Polym. Degrad. Stab.* **2005**, *88*, 473–479. [CrossRef]
33. Poletto, M.; Zattera, A.J.; Forte, M.M.; Santana, R.M. Thermal decomposition of wood: Influence of wood components and cellulose crystallite size. *Bioresour. Technol.* **2012**, *109*, 148–153. [CrossRef] [PubMed]
34. Stark, N.M.; Matuana, L.M. Surface chemistry changes of weathered HDPE/wood-flour composites studied by XPS and FTIR spectroscopy. *Polym. Degrad. Stab.* **2004**, *86*, 1–9. [CrossRef]
35. Marco, C.; Gómez, M.A.; Ellis, G.; Arribas, J.M. Activity of a β-nucleating agent for isotactic polypropylene and its influence on polymorphic transitions. *J. Appl. Polym. Sci.* **2002**, *86*, 531–539. [CrossRef]
36. Li, J.; Cheung, W.; Jia, D. A study on the heat of fusion of β-polypropylene. *Polymer* **1999**, *40*, 1219–1222. [CrossRef]
37. Guadagno, L.; D'Aniello, C.; Naddeo, C. Vittoria Polymorphism of Oriented Syndiotactic Polypropylene. *Macromolecules* **2000**, *33*, 6023–6030. [CrossRef]

38. Parenteau, T.; Ausias, G.; Grohens, Y.; Pilvin, P. Structure, mechanical properties and modelling of polypropylene for different degrees of crystallinity. *Polymer* **2012**, *53*, 5873–5884. [CrossRef]
39. Ferg, E.; Bolo, L. A correlation between the variable melt flow index and the molecular mass distribution of virgin and recycled polypropylene used in the manufacturing of battery cases. *Polym. Test.* **2013**, *32*, 1452–1459. [CrossRef]
40. Abdou, J.P.; Reynolds, K.J.; Pfau, M.R.; Van Staden, J.; Braggin, G.A.; Tajaddod, N.; Minus, M.; Reguero, V.; Vilatela, J.J.; Zhang, S. Interfacial crystallization of isotactic polypropylene surrounding macroscopic carbon nanotube and graphene fibers. *Polymer* **2016**, *91*, 136–145. [CrossRef]
41. Hirose, M.; Yamamoto, T.; Naiki, M. Crystal structures of the α and β forms of isotactic polypropylene: A Monte Carlo simulation. *Comput. Theor. Polym. Sci.* **2000**, *10*, 345–353. [CrossRef]
42. Varga, J.; Ehrenstein, G.W.; Schlarb, A.K. Vibration welding of alpha and beta isotactic polypropylenes: Mechanical properties and structure. *Express Polym. Lett.* **2008**, *2*, 148–156. [CrossRef]
43. Guerra, V.; Wan, C.; McNally, T. Nucleation of the β-polymorph in Composites of Poly(propylene) and Graphene Nanoplatelets. *J. Compos. Sci.* **2019**, *3*, 38. [CrossRef]
44. Staniewicz, L.; Vaudey, T.; Degrandcourt, C.; Couty, M.; Gaboriaud, F.; Midgley, P. Electron tomography provides a direct link between the Payne effect and the inter-particle spacing of rubber composites. *Sci. Rep.* **2014**, *4*, 7389. [CrossRef] [PubMed]
45. Rueda, M.M.; Fulchiron, R.; Martin, G.; Cassagnau, P. Rheology of polypropylene filled with short-glass fibers: From low to concentrated filled composites. *Eur. Polym. J.* **2017**, *93*, 167–181. [CrossRef]